Megapixel Infrared Arrays at the European Southern Observatory

G. Finger, P. Biereichel, J.L. Lizon, M. Meyer, A. F. M. Moorwood, G. Nicolini, and A. Silber

European Southern Observatory
Karl Schwarzschild Str. 2, 85748 Garching b. München, Germany.

ABSTRACT

For the next generation of instruments which will be used at 8 m telescopes large format arrays are needed. Better image quality obtained by adaptive optics requires sampling to higher spatial frequencies. The large field of these instruments increases the demand for array formats as large as 1024x1024 and beyond. For this reason ESO is committed to the development of megapixel infrared detectors. In a multimode instrument covering the 1 to 5 µm spectral range a detector has to fulfill very different requirements For high resolution spectroscopy low dark current and read noise are required. For broad band thermal imaging a high well capacity is needed to reduce the speed required to read out the array before it saturates. This paper gives a status report of ESO's activities related to large format arrays.

An ultrafast data acquisition system has been developed to read out large format arrays. The performance goal is to achieve shot noise limited operation in the wavelength region of λ =1 to 5 µm. The array controller is capable of handling the high data rates generated in the thermal infrared. The design of the controller was mainly driven by the requirement to read out the 32 parallel video channels of the SBRC 1024x1024 InSb detector in 50 msec. The array controller can also cope with the low read noise required for flux levels of < 1 photon/sec. A new test camera for large format arrays has also been built.

First test results obtained with the Rockwell 1024x1024 HgCdTe array are presented. The noise and dark current performance will be discussed with regard to OH line suppression. Read speed requirements will be defined for advanced readout techniques of image sharpening applying on chip tracking in the multiple nondestructive readout mode.

Keywords: infrared detector, infrared array, InSb, MCT, HgCdTe, megapixel, 1024x1024, HAWAII, ALADDIN

1.Introduction

In less than 10 years infrared arrays have evolved from formats of 58x62 pixels [1] to formats of 1024x1024, and their noise performance has improved by more than one order of magnitude.

At present two main projects of megapixel arrays are under development. For the wavelength range of 1 - 5 µm the ALADDIN project, the Advanced Large Area Detector Development in InSb, is an effort of the Santa Barbara Research Center, the National Optical Astronomy Observatory and the US Naval Observatory to develop a 1024x1024 InSb array [2] . The readout of the Aladdin array is organized in four independent quadrants. Each quadrant has eight parallel video outputs. The array can be read out with frame rates of 20 Hz. This read speed is required for broadband imaging in the thermal infrared in order to be able to read out the detector array before it is completely discharged by the high photon flux. ESO is planning to procure a small foundry run which will produce six sensor chip assemblies on a best effort basis. In order to handle the preprocessing of a continuous data rate of 20 megapixels/sec, we had to develop a completely new transputer based data acquisition system called IRACE. It relies on parallel processing using new T9000 processors.

The second array project covering the spectral range of 1 - 2.5 µm, is called HAWAII, the HgCdTe Astronomical Wide Area Infrared Imager [3] . It is a collaboration between Rockwell International Science Center and the University of Hawaii with funding provided by the Air Force Phillips Laboratory and led to the development of a 1024x1024 HgCdTe array having a cutoff wavelength of λ_c=2.5 µm. ESO has received an engineering grade array which has been under test for two months. It is the first array read out with the new data acquisition system IRACE and has been tested in the new test camera. First test results obtained with the engineering-grade array are presented below.

2.Data Acquisition System IRACE

The main design driver for the development of the Infrared Array Control Electronics IRACE was the SBRC 1024x1024 InSb array which generates frame rates of 20 Hz at 32 parallel video output channels. If 32 parallel 16 bit ADC's are used for digitizing the video signal a continuous data stream of 400 Mbit/sec has to be processed in real time. To provide the required CPU power parallel processing must be applied. The IRACE system is based on T9000 transputers and C104 link switches. It can be scaled to different processing needs and is programmed in OCCAM, a processing language specially developed for multiprocessor programming.

The IRACE data acquisition system consists of four main components, the detector board with differential line drivers, the data acquisition front end, the number cruncher and the workstation for system administration. The infrared array detector and the differential line drivers for the video signals are inside the cryostat. The detector front end is housing the following components: clock pattern generator; clock level converter and bias generator; analog to digital converters (500 nsec/16 bit) and a gigabit fiber optic link. It is placed close to the detector outside the cryostat. It is based on T8 transputers. An important design feature is the complete galvanic separation of the detector front end from the rest of the electronics by a gigabit fiber link for the digitized video signal and an Os fiber link for the T8 transputers [4]. Ground loops can thus be avoided which is mandatory for beating the noise levels of the video signal down to the 10 μV range.

The number cruncher receives the digitized video signal from the serial Gigabit fiber-optic link receiver. Data are put onto a high speed bus identical to the bus at the detector front end. Dma controllers on this bus distribute the data to the T9000 transputers for parallel real time processing of the video channels such as subtraction for double correlated sampling, averaging, updating of Gaussian sums for the least squares fit of the integration ramp in multiple nondestructive sampling mode, on chip tracking, real time flatfielding etc. The T9000 processors are organized in a tree-like structure. At the top of the tree one T9000 collects the different parts of the image, solves the error equations for calculation of the slopes of the integration ramp. Separate T9000 processors are used for fast real time display, for writing data to an array of SCSI disks in the raw data taking mode and for writing data to a SUN SPARC 10 workstation, which passes preprocessed images to the host workstation via FDDI. The SUN SPARC 10 also coordinates the T8 front end system and the T9000 number cruncher and is used for transputer software development. The SUN is a VME board residing in the VME crate of the number cruncher. The speed performance of IRACE which can be achieved for reading out the ALADDIN array is summarized in table 1. Clearly, the read speed will be limited by the detector which can be read out in 50 msec. At present a 4 channel version of IRACE is used for evaluation of the HAWAII array. IRACE will be expanded to a 32 channel version for reading out the ALADDIN array.

Table 1: Expected minimum readout times for a 32 channel 1024x1024 array using IRACE

Readout Mode	Readout time [msec]
uncorrelated with averaging	23
double correlated with averaging	46
multiple nondestructive sampling including least squares fit of integration ramp	43

3.Test Camera

To evaluate the performance of large format IR arrays in the lab and at the telescope a new test camera was built. The camera is an f/11 Offner design having 1:1 magnification. A drawing of the camera is shown in figure 1. It consists of two concentric spherical aluminum mirrors which are diamond turned and gold coated. The small mirror acts as a cold Lyot stop for thermal and stray light suppression. The camera has two cold filter wheels which are driven by cryogenic stepper motors. One filter wheel is equipped with bandpass filters, the other filter wheel with neutral density filters for simulation of the low flux levels typical in high resolution spectrographs. One of the filter positions is occupied by a focal reducer lens (f/11to f/2) for spot scans. The camera is cooled by a two stage closed cycle cooler. The first stage cools the optics to 80 K. To speed up cooldown, an additional continuous flow system for liquid nitrogen may be used. The second stage of the closed cycle cooler cools the detector to 20 K.

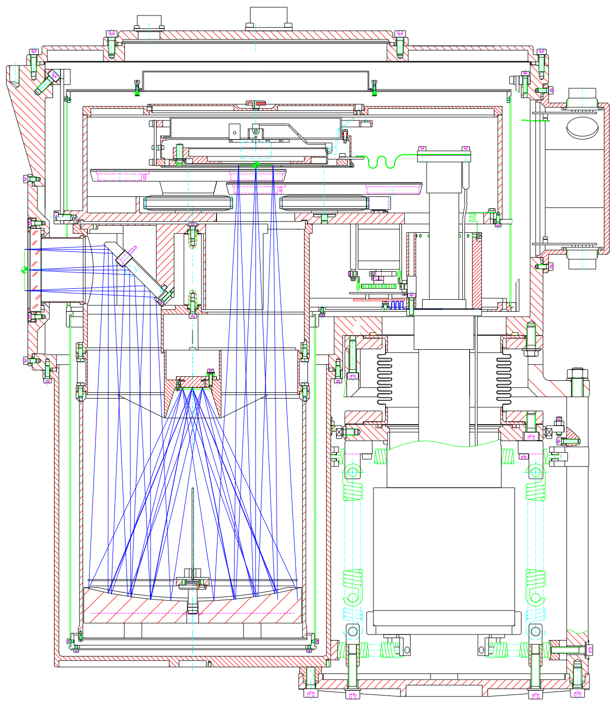

Figure 1 Test camera for large format arrays. f/11 Offner design with cold Lyot stop. Two filter wheels for bandpass and attenuation filters. Focal reducer f/11 to f/2 for spot scan of individual detector pixels.

4.Evaluation of 1024x1024 HgCdTe engineering grade array

The first megapixel IR array tested at ESO was an engineering grade HAWAII 1024x1024 HgCdTe array produced by Rockwell. The array has two quadrants of good cosmetic quality as can be seen in figure 7. One quadrant is light sensitive and one quadrant is defective. The array has been under test since April 1996. First test results will be presented in the following paragraph.

4.1.Gain Calibration

The gain of the data acquisition chain was calibrated by measuring the shot noise as a function of detector signal at high photon flux levels where the photon shot noise dominates the detector readout noise. In figure 2 the variance of the detector signal is plotted versus the detector signal. The inverse slope of the regressional line fitted to the measured data points yields the pixel transfer function in units of electrons/ADU. By this method the gain of 2.97 electrons/ADU has been determined completely independent of any system gain. The voltage gain of the two-stage on-chip source follower was measured by keeping the reset switch permanently closed during the detector readout, while changing the external detector bias voltage and observing the dc level shift of the video output. A voltage gain of 0.686 has been determined at a temperature of 65 K. In our setup 1 ADU corresponds to 9.53 µV at the video output of the detector. From the measured pixel transfer function of 2.93 e/ADU and the measured voltage gain of the complete signal chain the capacity of the integrating node can be retrieved. It is 34 fF at an external bias voltage of - 0.5 V. The value quoted by the manufacturer is 20 fF and was measured at a reverse bias voltage of -1V. This discrepancy may be due to the voltage dependence of the diode capacity as given by equation (EQ 1).

$$C(V) = A_{Diode}\sqrt{\frac{\varepsilon_{InSb} N_{doping} e}{2\left(V_{builtin} + V\right)}} + C_{Gate} \qquad \text{(EQ 1)}$$

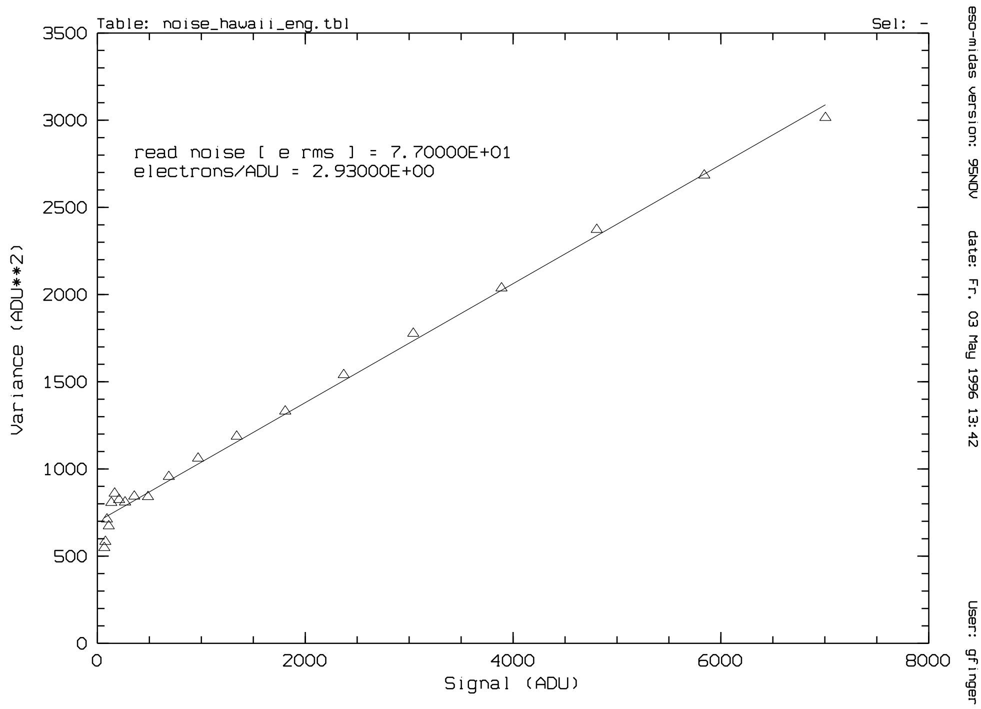

Figure 2 : Pixel transfer function of Rockwell 1024x1024 HgCdTe array. PTF = 2.93 e/ADU at 0.5 V external reverse bias.

4.2.Quantum Efficiency

Knowing the gain of the data acquisition system, the quantum efficiency of the detector can be determined with a calibrated radiation source. The detector integration time was set to 2.5 sec, and a variable temperature blackbody source was used. The array was uniformly illuminated by the blackbody. Intervening optical materials were a BaF_2 cryostat window, a cooled bandpass and an optional neutral density filter. The transmission of the band pass filters and the neutral density filters have been measured at liquid nitrogen temperature. They have been carefully checked for radiation leaks over the complete 1 to 2.5 µm spectral range. The blackbody was chopped synchronously with the detector readout in order to eliminate fluctuations of laboratory background radiation. The photon flux was varied by changing the blackbody temperature. The same bias voltage of 500mV used for retrieving the pixel transfer function was applied during quantum efficiency measurements. This is essential, since the PTF changes during the ongoing integration as do the depletion width and the capacity of the detector diode. Only one third of the well was filled. Hence, the integration ramp can be considered linear with reasonable accuracy. An example for the K band measurement is shown in figure 3. The measured overall QE is 64% in K and uniform across the array. The QE is the average of all detector pixels. Quantum efficiencies in the J and H band have been determined in a similar way, but a different high temperature blackbody was used which illuminates only a part of the array. The results of quantum efficiency measurements are summarized in Table 2. The QE values were obtained at a detector temperature of 55 K.

Table 2: Quantum efficiency of Rockwell 1024x1024 HgCdTe array at 55 K

bandpass	QE
J	0.65
H	0.65
K	0.64

4.3.Dark Current

Great care was taken to measure the dark current of the detector, which is one of the key parameters for low background applications in high resolution spectrographs. The sky brightness in the near infrared is dominated by narrow OH emission lines. Noise and dark current characteristics of the detector may decide which is the best way to reduce the sky background of low resolution spectra. Either a special OH line suppression spectrograph has to be built to mask the OH lines, or the high resolution spectrum can be digitally recombined from spectral regions unaffected by the OH lines, the latter requiring a detector with extremely low dark current and read noise.

The dark current was measured by repeated nondestructive readouts of a single integration ramp lasting several hours. Prior to each measurement the detector was reset 128 times. After the reset the detector needs several seconds to settle before the integration ramp becomes linear. Immediately after the reset the detector signal was sampled in shorter time intervals. After one hour a nondestructive readout was performed every hour. An example of the integration ramp for a dark exposure is shown in figure 2. The buffered output of the on chip source follower was used. The output source follower was not switched off during the stare time when the detector was not being read out. At a detector temperature of 50 K the dark current is 0.25 e/sec. The glow caused by electroluminescence of the Si multiplexer is confined to the corners of the array quadrants, where the buffer amplifiers are located. It is 5.5 e/sec and mainly caused by amplifier glow. Since the dark current decreases from 8.7 e/sec to 0.25 e/sec when the detector is cooled from 80 K to 50 K, a complete temperature scan of the dark current was carried out and is shown in figure 2. The temperature dependence at 50 K is $\propto \exp(-T_{eff}/T) \propto \exp(-E_g/mKT)$ and can be characterized by an effective temperature T_{eff}=132 K which is equivalent to a very small activation energy E_g/m, with m being m=43.6. The dark current mechanism is unclear. It has been demonstrated that the amplifier glow can be reduced by using off-chip JFET's directly connected to the unbuffered output bypassing the on-chip source follower [5] . Figure 7 shows a dark exposure which is normalized to a dark current in units of e/sec. It was obtained from the difference of two nondestructive readouts taken 1750 and 8990 sec after reset. Since the glow is confined to the regions close to the output amplifiers and the dark current exhibits a strong temperature dependence it seems reasonable to suspect that glow is not dominating our dark current measurements. But further investigations using external JFET's will be carried out.

4.4.Readout Noise

First noise tests applying double correlated sampling have been performed with a large analog bandwidth of the data acquisition system. The rise time of the system was 270 nsec. This is faster than the buffered video output of the on-chip source follower which has a rise time of 3 µsec. The rms noise of 32 consecutive double correlated readouts was 24 e rms, which includes the noise of both readouts of the double correlated clamp. Dark exposures of 2.5 sec were used. This result is based on the measured integrating node capacity of 34 fF and not on the value of 20fF as quoted by the manufacturer. Our setup is still susceptible to noise pickup from the cryostat environment and shielding must be further improved.

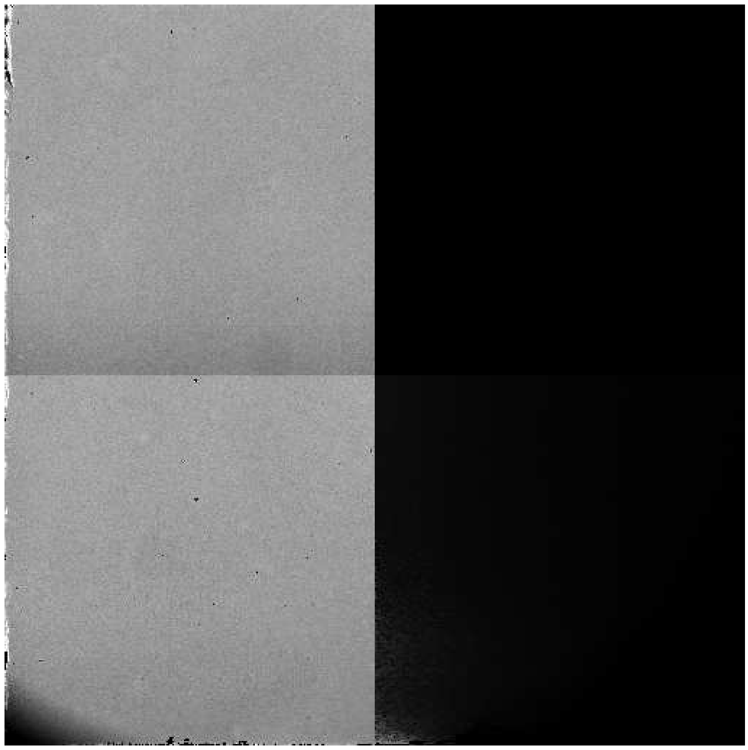

Figure 3 : K band quantum efficiency of Rockwell 1024x1024 HgCdTe array. Cut levels = 0 , 1. Mean QE is 64%.

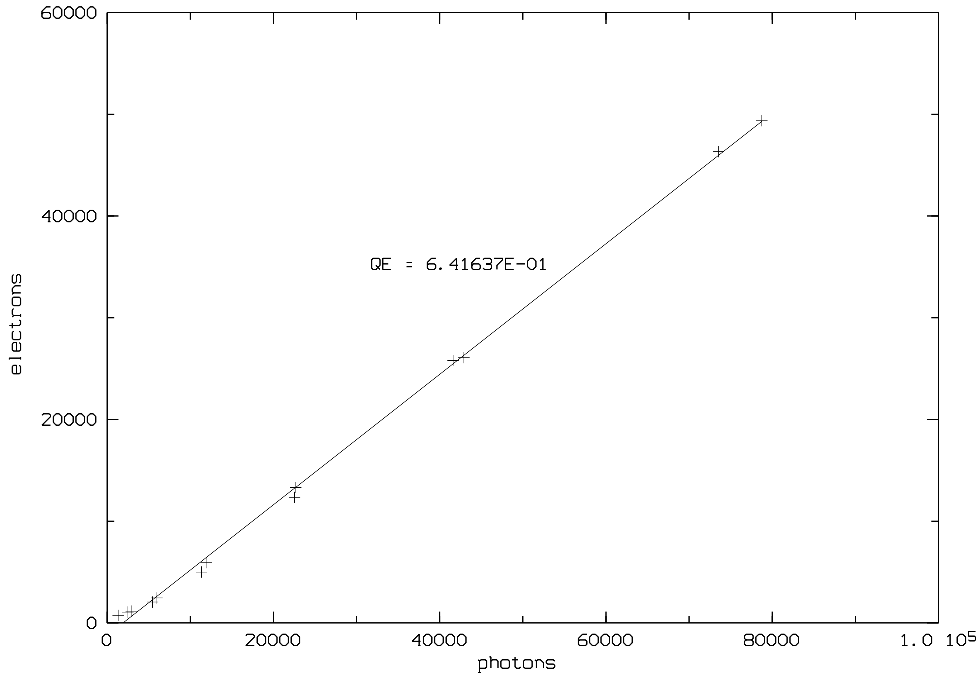

Figure 4 : Photometric quantum efficiency calibration of Rockwell 1024x1024 HgCdTe array in K band. Detector integration times 1 sec and 2 sec. External reverse bias voltage 500 mV.

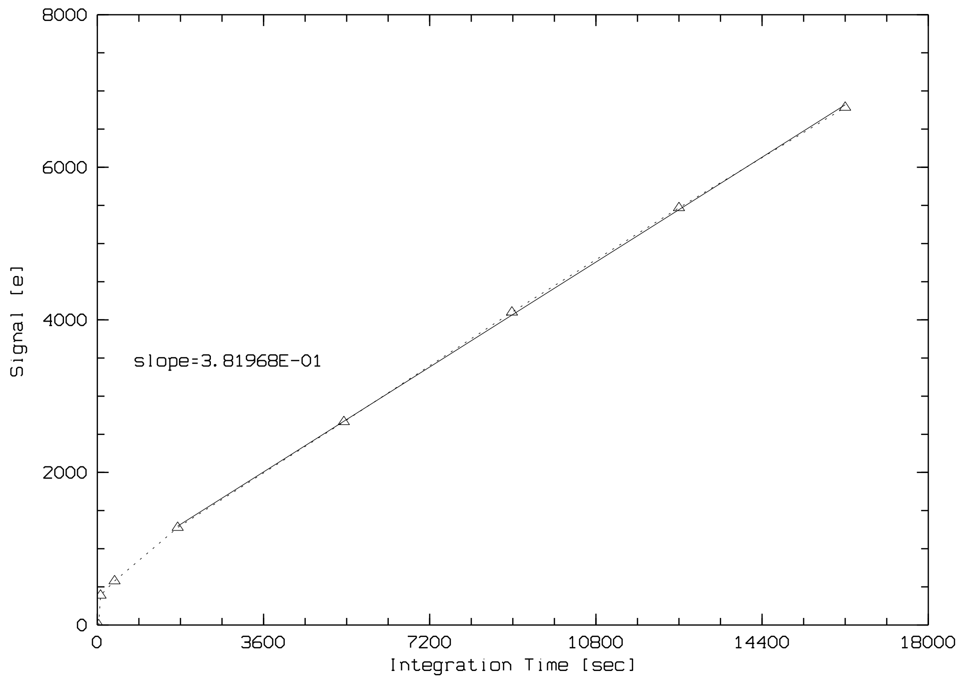

Figure 5 : Detector Signal versus time for a dark exposure at 55 K. Dark current is 0.38 e/sec.

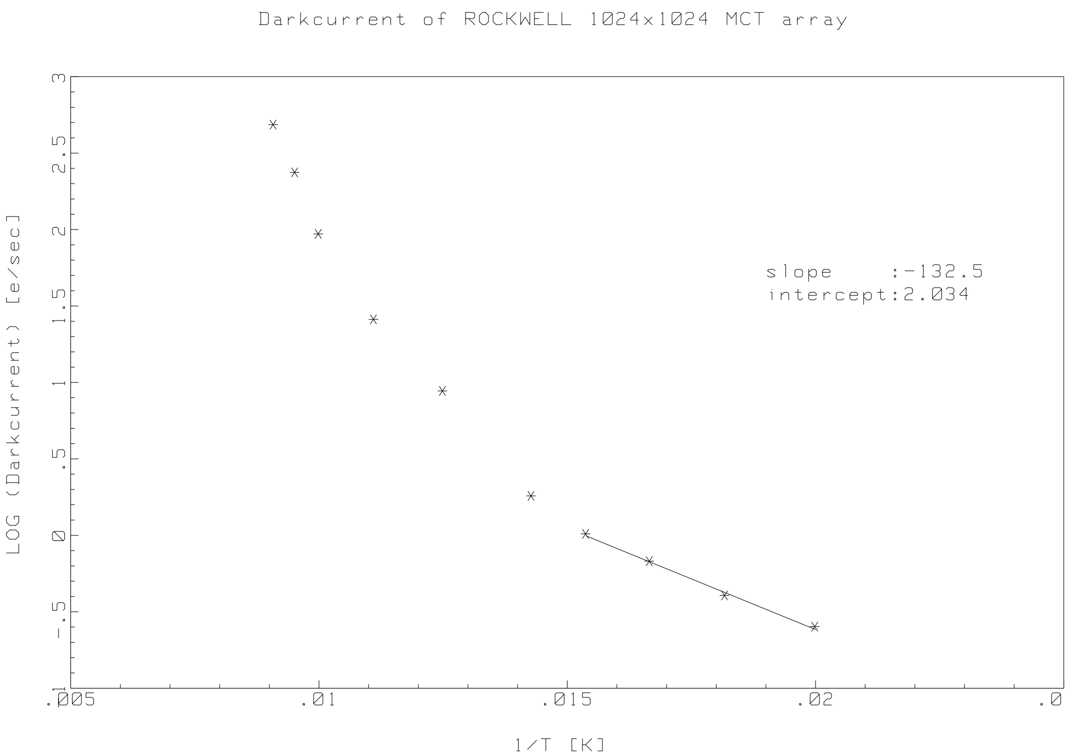

Figure 6 : Temperature dependence of dark current. Effective temperature at 50 K is T_{eff}=132 K.

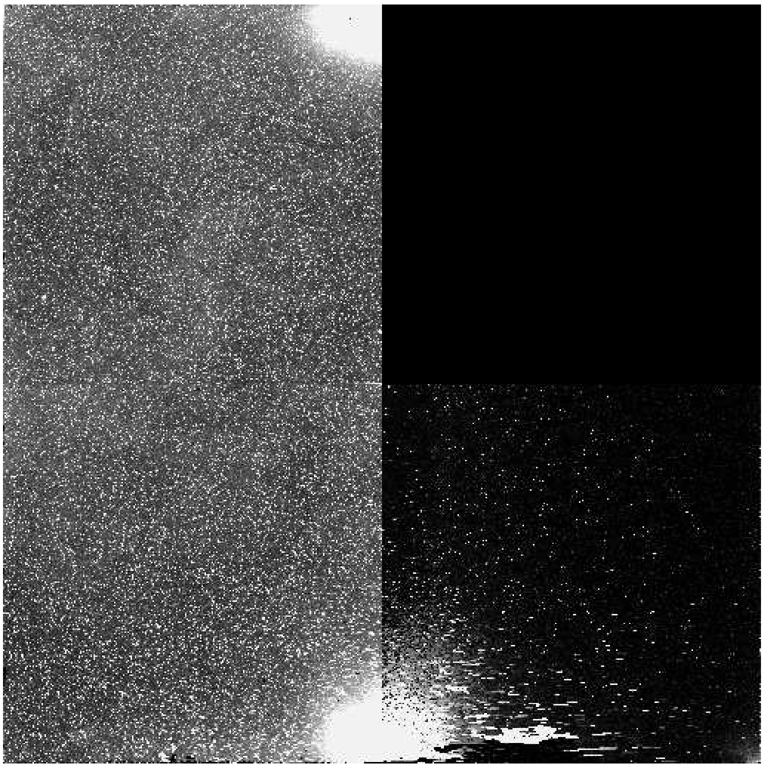

Figure 7 : Dark current of HAWAII 1024x1024 HgCdTe array. Low cut = 0 e/sec. High cut = 0.5 e/sec. Electroluminescence is confined to the corners of the quadrants.

In the multiple nondestructive sampling mode applying a least squares fit to 80 nondestructive readouts of the integration ramp of 2 minute dark exposures the readout noise could be reduced to 12 e rms in regions of the array at some distance from the buffer amplifiers and shift registers. Further tests are planned matching the analog bandwidth of the acquisition chain to the speed of the detector. External JFET's will be used bypassing the on-chip buffer output.

With measured readout noise and dark current figures of the HAWAII detector tested here, H band spectra having a spectral resolution R=2500 will be limited by the shot noise of the dark current and not by the readout noise, as soon as the detector integration becomes larger than 10 minutes. Simulations of both long slit spectrographs and integral field spectrometers predict for the OII line of a galaxy at z=2 a signal to noise improvement of a factor of 2 if the dark current is reduced from 900 e/sec/hour to 200 e/sec/hour.

4.5.Persistence

If the detector field of view contains a bright radiation source the subsequent dark exposures exhibit residual excess dark current of those pixels onto which the bright source had been imaged in the previous exposure. This persistence effect of the HAWAII device is strongly reduced in comparison to the NICMOS 3 array, the predecessor of the HAWAII detector [6] . The persistence effect is not completely eliminated in the HAWAII detector as demonstrated by a series of specific tests. In these tests a point source was imaged onto the detector and generated a total photocurrent of 2.2 10^5 e/sec. In the first subsequent 1 minute dark exposure the photocurrent was reduced to 200 e/sec. The second 1 minute dark exposure did not show any measurable residual excess dark current above the noise level of 10 e/sec.

4.6.Spot Scan

The sensitivity profile of a single pixel is required for modelling the overall MTF of the instrument including optics and detector. It helps the instrument designer to define the required optical quality. If the sensitivity profile of a single detector pixel is accurately known the mechanisms which reduce the quantum efficiency of the detector can be separated. The slope of the sensitivity profile yields the diffusion length of the minority carriers of the detector material. For these reasons a special effort was undertaken to produce an infrared spot which is small compared to the pixel size of 18.5 µm and can be used for spot scans of single pixels. Since the diameter of the airy disk is $2.44\lambda f^{\#}$ the f/11 Offner camera produces diffraction limited images which are larger than the pixel size. For this reason a special focal reducer lens f/11 to f/2 has been fabricated to produce light spots smaller than the pixel size. The lens had to fit in the converging beam of the f/11 Offner camera and occupies one of the filter wheel positions. The lens functions as substrate for the reflecting surfaces. The entrance and output surfaces of the lens are concentric to the object plane which is the detector surface. Therefore, the lens is totally achromatic independent of the detector material. The principle of the lens is a solid inverse cassegrain telescope. Figure 2 shows the first spot scan performed with this lens. The response of five adjacent pixels in a row is plotted versus spot position. The maxima of the response curves decrease from pixel to pixel because the scan direction is not parallel to the detector row. The upper curve is the total integrated intensity of all pixels. The next neighbors of the brightest pixel contain 15% of the signal measured on the central pixel. The energy concentrated on the central pixel is 60% of the total energy. The spot scan is probably a convolution of the optical spot profile and the detector response. The quoted values are worst case limits and further improvement of the optical alignment is necessary; This is difficult since the alignment has to be checked with pixels much larger than the optical spot diameter. The sensitivity profile of the detector is mainly determined by the diffusion length of the minority carriers. The location where the photon generates the signal charge is dependent on the absorption coefficient of the IR active material. The electron hole pair has to diffuse to the pn junction where it is separated by the electric field of the depletion region. Since the width of the depletion region depends on the bias voltage, the sensitivity profile may depend on the bias voltage.

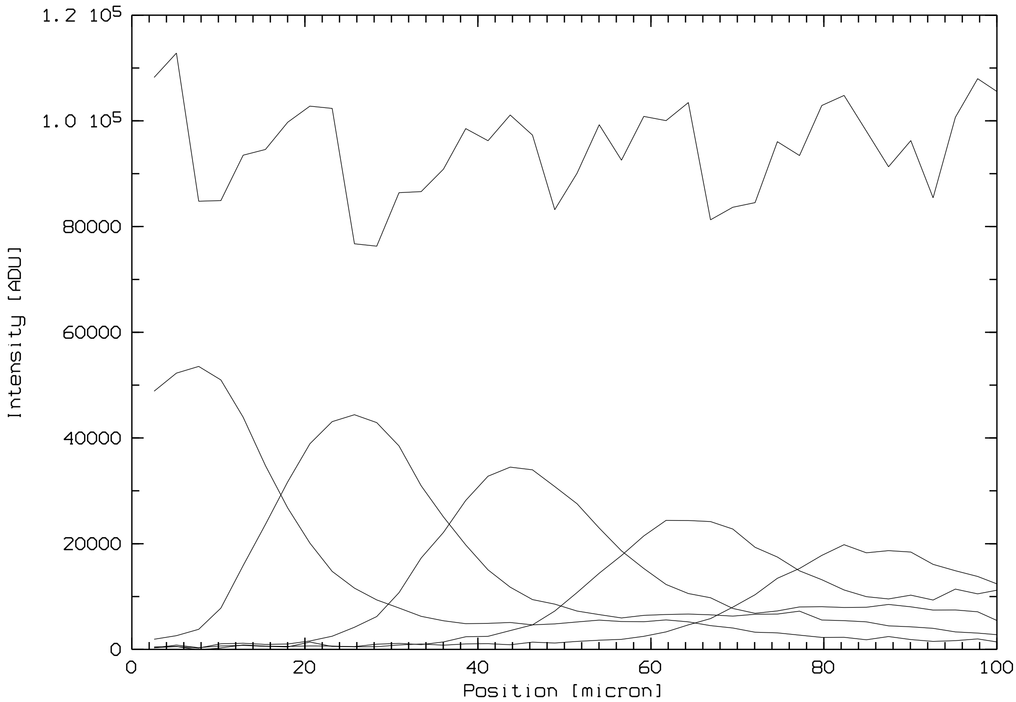

Figure 8 : Spot scan of HAWAII array.

4.7.Read speed and image sharpening

The low noise, low dark current and high quantum efficiency achieved with the HAWAII array open up new applications of the device as IR wavefront sensor [5] . Furthermore, at telescope foci without adaptive optics and tip tilt mirrors image sharpening can be achieved by on-chip tracking techniques [7] . In the multiple nondestructive readout mode the difference of two consecutive nondestructive readouts is a short time exposure with an integration time equal to the sampling interval. These short time exposures can be recentered to compensate for image motion induced by atmospheric turbulence. The time interval between two nondestructive readouts must be at least as long as the readout time τ of the array which is the critical parameter for these applications. To estimate the readout time τ required for the correction of image motion, a power spectral density of atmospheric tilt was used which is based on measured height profiles of wind speed and temperature turbulence coefficients C_T^2 [8] . In order to retrieve the phase variance of an image obtained from recentered differences of nondestructive readouts of integration time τ, the power spectral density must be multiplied by the filter function $1-(\sin(\pi\tau f)/\pi\tau f)^2$ and integrated over all frequencies f. An expression given by Parenti et al. [9] allows to convert the tilt corrected phase variance to Strehl ratios of images obtained with the on-chip tracking algorithm. For the multimode infrared instrument SOFI, which will be installed at the 3.5 m NTT telescope in LaSilla, the dependence of Strehl ratio on readout time τ achievable with on-chip tracking was calculated assuming typical seeing conditions of FWHM = 0.5 arcsec at λ = 0.5 µm and a wind speed of v = 5 m/sec. The result is shown in figure 9. Without any optimization we have been able to read the array with 3 µs address time per pixel. If all four quadrants are read out in parallel, this corresponds to a readout time of τ = 750 msec. In order to increase the speed of the output driver one can adjust the bias gate voltage from the nominal 3.5V setting towards ground. This will increase the current to the drive circuit. Unfortunately, one has to pay a dynamic range penalty for doing this. To overcome this problem one can adjust the detector substrate below ground. Further, the output source follower can be made faster by decreasing its pullup resistor. Experiments are ongoing, and we hope that a combination of these adjustments will enable us to do readouts faster. If the address time per pixel can be reduced to 1 µs the complete array can be read out in 250 msec. This would increase the Strehl ratio of K band images corrected by the on-chip tracking algorithm from 0.27 to 0.43.

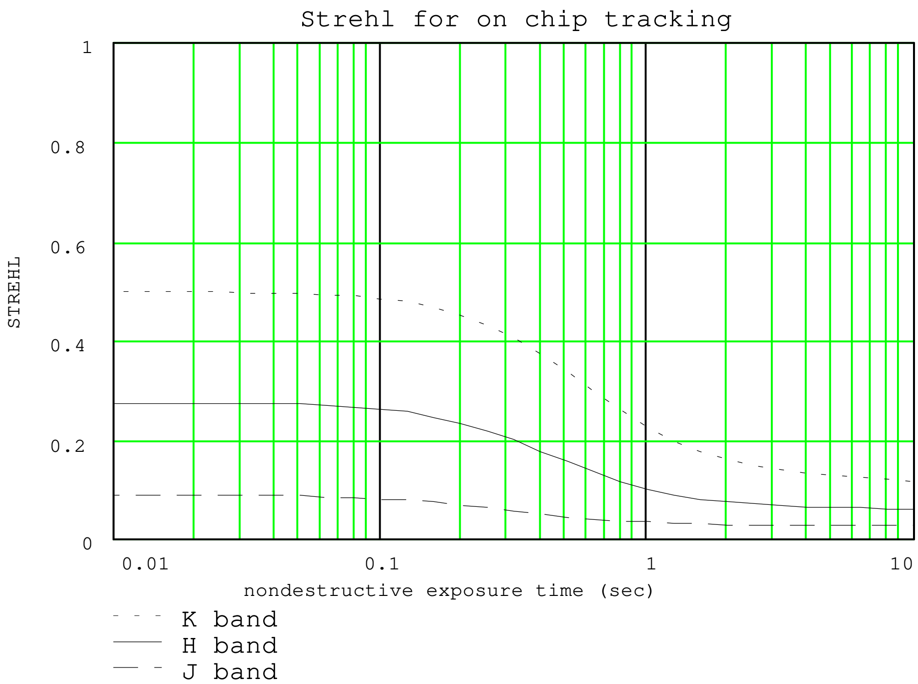

Figure 9 Strehl ratio of images corrected by on-chip tracking showing dependency on detector readout time τ for J, H and K band. Assumptions: telescope diameter 3.5 m, FWHM = 0.5 arcsec at λ = 0.5 µm, wind speed of v = 5 m/sec.

5.Conclusions

Megapixel IR arrays have become available and are under active investigation. The performance of an engineering grade HAWAII 1024x1024 HgCdTe array produced by Rockwell International Science Center has been evaluated in our new test camera. The array was operated by IRACE, our new ultrafast transputer based data acquisition system. The dark current of the HAWAII array is temperature dependent and 0.25e/sec at 50 K. Some of the problems such as amplifier glow and persistence encountered with NICMOS-3 arrays, the predecessor of the HAWAII array, have been substantially reduced. Readout noise of 12 e rms could be achieved but further improvements may be possible by better shielding and by using external JFET's bypassing the on chip amplifier. Readout times of 750 msec have been demonstrated. Experiments to reduce the readout time are in progress in order to increase the effectiveness of first order corrections of wavefront distortions induced by atmospheric seeing.

Our data acquisition system will be expanded to a 32 channel version for testing 1024x1024 InSb arrays produced by Santa Barbara Research Center. Large format 1Kx1K arrays are not yet off the shelf devices. However, plans already exist to extend the PACE-1 technology of HgCdTe to formats of 2Kx2K. Infrared focal plane technology is still rapidly developing and will expand the frontiers of IR astronomy.

6.Acknowledgements

The authors wish to thank B. Delabre, B. Köhler, L. Nöethe, A. van Dijsseldonk and O von der Lühe for their support and helpful discussions.

7.References

[1]A. M. Fowler, R. G. Probst, J.P. Britt, R. R. Joyce, F.C. Gillet, “Evaluation of an InSb Hybrid Focal Plane Array for Ground-based Astronomy”, Optical Engineering 26, 3, pp. 232-240, 1987.

[2]A. M. Fowler, I. Gatley, F.J. Vrba, H.D.Ables, A. Hoffman and J. Woolaway, “Aladdin, the 1024x1024 InSb Array: Test Results”, Proceedings SPIE 2475, pp. 27-33, 1995.

[3]L.J. Kozlowski, K. Vural, S.A.Cabelli, C.Y. Chen, D.E. Cooper, G.L Bostrup, D.M. Stephenson, W.L. McLevige, R.B.Bailey, K. Hodapp, D.Hall and W.E. Kleinhans, “2.5 µm PACE-I HgCdTe 1024x1024 FPA for Infrared Astronomy”, Proceedings SPIE 2268, pp. 353, 1994.

[4]M. Meyer, G. Finger and H. Mehrgan, “Connection between detector front end and number cruncher with 1 Gbit/s multiplexing fiber-optic link”, Proceedings SPIE 2475, pp. 97-104, 1995.

[5]K.W.Hodapp, J.L.Hora, L.L.Cowie, M.Metzger, E.Irwin, D.Hall, K. Vural, L.J. Kozlowski, S.A.Cabelli, C.Y. Chen, D.E. Cooper, G.L Bostrup, R.B. Bailey, W.E. Kleinhans, “The Hawaii Infrared Arrays: Testing and Astronomical Characterization of Prototype and Science-Grade Devices”, to be published in New Astronomy.

[6]G. Finger, P Biereichel, M. Meier and A.F.M. Moorwood, “Image Sharpening by On-Chip Tracking in IRAC2”, Proceedings SPIE 1946, pp. 134-145, 1993.

[7]G. Finger, P Biereichel, A. van Dijsseldonk, M. Meier and A.F.M. Moorwood, “Real Time Image Sharpening without Adaptive Optics by On-Chip Tracking”, Proceedings SPIE 2198, pp. 763-773, 1994.

[8]O. von der Lühe, M. Sarazin, “Power Spectral Densities of Atmospheric Image Wander at Paranal“, ESO Report VLT-TEL-92/2064, 1993.

[9]R.R. Parenti and R.J. Sasiela, “Laser-guide-star systems for astronomical applications”. Opt. Soc. Am., Vol 11, pp 288-309,1994.

Megapixel Infrared Arrays at the European Southern Observatory

G. Finger, P. Biereichel, J.L. Lizon, M. Meyer, A. F. M. Moorwood, G. Nicolini, and A. Silber

European Southern Observatory
Karl Schwarzschild Str. 2, 85748 Garching b. München, Germany.

ABSTRACT

For the next generation of instruments which will be used at 8 m telescopes large format arrays are needed. Better image quality obtained by adaptive optics requires sampling to higher spatial frequencies. The large field of these instruments increases the demand for array formats as large as 1024x1024 and beyond. For this reason ESO is committed to the development of megapixel infrared detectors. In a multimode instrument covering the 1 to 5 µm spectral range a detector has to fulfill very different requirements For high resolution spectroscopy low dark current and read noise are required. For broad band thermal imaging a high well capacity is needed to reduce the speed required to read out the array before it saturates. This paper gives a status report of ESO's activities related to large format arrays.

An ultrafast data acquisition system has been developed to read out large format arrays. The performance goal is to achieve shot noise limited operation in the wavelength region of λ =1 to 5 µm. The array controller is capable of handling the high data rates generated in the thermal infrared. The design of the controller was mainly driven by the requirement to read out the 32 parallel video channels of the SBRC 1024x1024 InSb detector in 50 msec. The array controller can also cope with the low read noise required for flux levels of < 1 photon/sec. A new test camera for large format arrays has also been built.

First test results obtained with the Rockwell 1024x1024 HgCdTe array are presented. The noise and dark current performance will be discussed with regard to OH line suppression. Read speed requirements will be defined for advanced readout techniques of image sharpening applying on chip tracking in the multiple nondestructive readout mode.

Keywords: infrared detector, infrared array, InSb, MCT, HgCdTe, megapixel, 1024x1024, HAWAII, ALADDIN

1.Introduction

In less than 10 years infrared arrays have evolved from formats of 58x62 pixels [1] to formats of 1024x1024, and their noise performance has improved by more than one order of magnitude.

At present two main projects of megapixel arrays are under development. For the wavelength range of 1 - 5 µm the ALADDIN project, the Advanced Large Area Detector Development in InSb, is an effort of the Santa Barbara Research Center, the National Optical Astronomy Observatory and the US Naval Observatory to develop a 1024x1024 InSb array [2] . The readout of the Aladdin array is organized in four independent quadrants. Each quadrant has eight parallel video outputs. The array can be read out with frame rates of 20 Hz. This read speed is required for broadband imaging in the thermal infrared in order to be able to read out the detector array before it is completely discharged by the high photon flux. ESO is planning to procure a small foundry run which will produce six sensor chip assemblies on a best effort basis. In order to handle the preprocessing of a continuous data rate of 20 megapixels/sec, we had to develop a completely new transputer based data acquisition system called IRACE. It relies on parallel processing using new T9000 processors.

The second array project covering the spectral range of 1 - 2.5 µm, is called HAWAII, the HgCdTe Astronomical Wide Area Infrared Imager [3] . It is a collaboration between Rockwell International Science Center and the University of Hawaii with funding provided by the Air Force Phillips Laboratory and led to the development of a 1024x1024 HgCdTe array having a cutoff wavelength of λ_c=2.5 µm. ESO has received an engineering grade array which has been under test for two months. It is the first array read out with the new data acquisition system IRACE and has been tested in the new test camera. First test results obtained with the engineering-grade array are presented below.

2.Data Acquisition System IRACE

The main design driver for the development of the Infrared Array Control Electronics IRACE was the SBRC 1024x1024 InSb array which generates frame rates of 20 Hz at 32 parallel video output channels. If 32 parallel 16 bit ADC's are used for digitizing the video signal a continuous data stream of 400 Mbit/sec has to be processed in real time. To provide the required CPU power parallel processing must be applied. The IRACE system is based on T9000 transputers and C104 link switches. It can be scaled to different processing needs and is programmed in OCCAM, a processing language specially developed for multiprocessor programming.

The IRACE data acquisition system consists of four main components, the detector board with differential line drivers, the data acquisition front end, the number cruncher and the workstation for system administration. The infrared array detector and the differential line drivers for the video signals are inside the cryostat. The detector front end is housing the following components: clock pattern generator; clock level converter and bias generator; analog to digital converters (500 nsec/16 bit) and a gigabit fiber optic link. It is placed close to the detector outside the cryostat. It is based on T8 transputers. An important design feature is the complete galvanic separation of the detector front end from the rest of the electronics by a gigabit fiber link for the digitized video signal and an Os fiber link for the T8 transputers [4] . Ground loops can thus be avoided which is mandatory for beating the noise levels of the video signal down to the 10 μV range.

The number cruncher receives the digitized video signal from the serial Gigabit fiber-optic link receiver. Data are put onto a high speed bus identical to the bus at the detector front end. Dma controllers on this bus distribute the data to the T9000 transputers for parallel real time processing of the video channels such as subtraction for double correlated sampling, averaging, updating of Gaussian sums for the least squares fit of the integration ramp in multiple nondestructive sampling mode, on chip tracking, real time flatfielding etc. The T9000 processors are organized in a tree-like structure. At the top of the tree one T9000 collects the different parts of the image, solves the error equations for calculation of the slopes of the integration ramp. Separate T9000 processors are used for fast real time display, for writing data to an array of SCSI disks in the raw data taking mode and for writing data to a SUN SPARC 10 workstation, which passes preprocessed images to the host workstation via FDDI. The SUN SPARC 10 also coordinates the T8 front end system and the T9000 number cruncher and is used for transputer software development. The SUN is a VME board residing in the VME crate of the number cruncher. The speed performance of IRACE which can be achieved for reading out the ALADDIN array is summarized in table 1. Clearly, the read speed will be limited by the detector which can be read out in 50 msec. At present a 4 channel version of IRACE is used for evaluation of the HAWAII array. IRACE will be expanded to a 32 channel version for reading out the ALADDIN array.

Table 1: Expected minimum readout times for a 32 channel 1024x1024 array using IRACE

Readout Mode	Readout time [msec]
uncorrelated with averaging	23
double correlated with averaging	46
multiple nondestructive sampling including least squares fit of integration ramp	43

3.Test Camera

To evaluate the performance of large format IR arrays in the lab and at the telescope a new test camera was built. The camera is an f/11 Offner design having 1:1 magnification. A drawing of the camera is shown in figure 1. It consists of two concentric spherical aluminum mirrors which are diamond turned and gold coated. The small mirror acts as a cold Lyot stop for thermal and stray light suppression. The camera has two cold filter wheels which are driven by cryogenic stepper motors. One filter wheel is equipped with bandpass filters, the other filter wheel with neutral density filters for simulation of the low flux levels typical in high resolution spectrographs. One of the filter positions is occupied by a focal reducer lens (f/11to f/2) for spot scans. The camera is cooled by a two stage closed cycle cooler. The first stage cools the optics to 80 K. To speed up cooldown, an additional continuous flow system for liquid nitrogen may be used. The second stage of the closed cycle cooler cools the detector to 20 K.

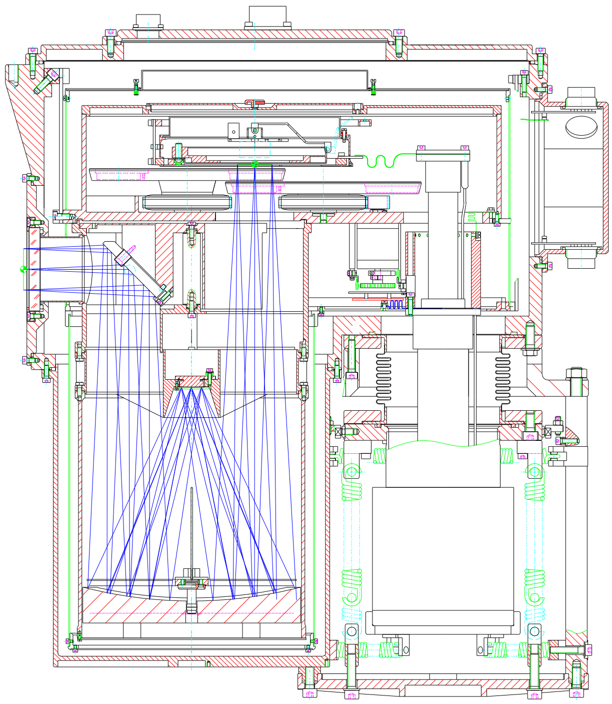

Figure 1 Test camera for large format arrays. f/11 Offner design with cold Lyot stop. Two filter wheels for bandpass and attenuation filters. Focal reducer f/11 to f/2 for spot scan of individual detector pixels.

4.Evaluation of 1024x1024 HgCdTe engineering grade array

The first megapixel IR array tested at ESO was an engineering grade HAWAII 1024x1024 HgCdTe array produced by Rockwell. The array has two quadrants of good cosmetic quality as can be seen in figure 7. One quadrant is light sensitive and one quadrant is defective. The array has been under test since April 1996. First test results will be presented in the following paragraph.

4.1.Gain Calibration

The gain of the data acquisition chain was calibrated by measuring the shot noise as a function of detector signal at high photon flux levels where the photon shot noise dominates the detector readout noise. In figure 2 the variance of the detector signal is plotted versus the detector signal. The inverse slope of the regressional line fitted to the measured data points yields the pixel transfer function in units of electrons/ADU. By this method the gain of 2.97 electrons/ADU has been determined completely independent of any system gain. The voltage gain of the two-stage on-chip source follower was measured by keeping the reset switch permanently closed during the detector readout, while changing the external detector bias voltage and observing the dc level shift of the video output. A voltage gain of 0.686 has been determined at a temperature of 65 K. In our setup 1 ADU corresponds to 9.53 µV at the video output of the detector. From the measured pixel transfer function of 2.93 e/ADU and the measured voltage gain of the complete signal chain the capacity of the integrating node can be retrieved. It is 34 fF at an external bias voltage of - 0.5 V. The value quoted by the manufacturer is 20 fF and was measured at a reverse bias voltage of -1V. This discrepancy may be due to the voltage dependence of the diode capacity as given by equation (EQ 1).

$$C(V) = A_{Diode}\sqrt{\frac{\varepsilon_{InSb} N_{doping} e}{2\left(V_{builtin} + V\right)}} + C_{Gate} \qquad \text{(EQ 1)}$$

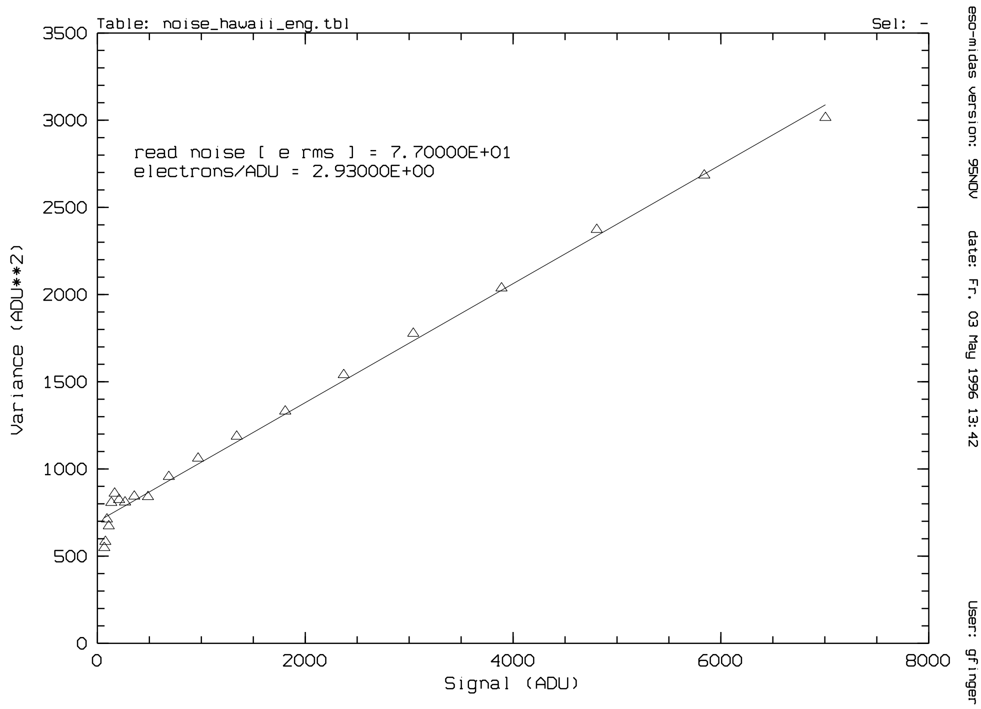

Figure 2 : Pixel transfer function of Rockwell 1024x1024 HgCdTe array. PTF = 2.93 e/ADU at 0.5 V external reverse bias.

4.2.Quantum Efficiency

Knowing the gain of the data acquisition system, the quantum efficiency of the detector can be determined with a calibrated radiation source. The detector integration time was set to 2.5 sec, and a variable temperature blackbody source was used. The array was uniformly illuminated by the blackbody. Intervening optical materials were a BaF_2 cryostat window, a cooled bandpass and an optional neutral density filter. The transmission of the band pass filters and the neutral density filters have been measured at liquid nitrogen temperature. They have been carefully checked for radiation leaks over the complete 1 to 2.5 µm spectral range. The blackbody was chopped synchronously with the detector readout in order to eliminate fluctuations of laboratory background radiation. The photon flux was varied by changing the blackbody temperature. The same bias voltage of 500mV used for retrieving the pixel transfer function was applied during quantum efficiency measurements. This is essential, since the PTF changes during the ongoing integration as do the depletion width and the capacity of the detector diode. Only one third of the well was filled. Hence, the integration ramp can be considered linear with reasonable accuracy. An example for the K band measurement is shown in figure 3. The measured overall QE is 64% in K and uniform across the array. The QE is the average of all detector pixels. Quantum efficiencies in the J and H band have been determined in a similar way, but a different high temperature blackbody was used which illuminates only a part of the array. The results of quantum efficiency measurements are summarized in Table 2. The QE values were obtained at a detector temperature of 55 K.

Table 2: Quantum efficiency of Rockwell 1024x1024 HgCdTe array at 55 K

bandpass	QE
J	0.65
H	0.65
K	0.64

4.3.Dark Current

Great care was taken to measure the dark current of the detector, which is one of the key parameters for low background applications in high resolution spectrographs. The sky brightness in the near infrared is dominated by narrow OH emission lines. Noise and dark current characteristics of the detector may decide which is the best way to reduce the sky background of low resolution spectra. Either a special OH line suppression spectrograph has to be built to mask the OH lines, or the high resolution spectrum can be digitally recombined from spectral regions unaffected by the OH lines, the latter requiring a detector with extremely low dark current and read noise.

The dark current was measured by repeated nondestructive readouts of a single integration ramp lasting several hours. Prior to each measurement the detector was reset 128 times. After the reset the detector needs several seconds to settle before the integration ramp becomes linear. Immediately after the reset the detector signal was sampled in shorter time intervals. After one hour a nondestructive readout was performed every hour. An example of the integration ramp for a dark exposure is shown in figure 2. The buffered output of the on chip source follower was used. The output source follower was not switched off during the stare time when the detector was not being read out. At a detector temperature of 50 K the dark current is 0.25 e/sec. The glow caused by electroluminescence of the Si multiplexer is confined to the corners of the array quadrants, where the buffer amplifiers are located. It is 5.5 e/sec and mainly caused by amplifier glow. Since the dark current decreases from 8.7 e/sec to 0.25 e/sec when the detector is cooled from 80 K to 50 K, a complete temperature scan of the dark current was carried out and is shown in figure 2. The temperature dependence at 50 K is $\propto \exp(-T_{eff}/T) \propto \exp(-E_g/mKT)$ and can be characterized by an effective temperature T_{eff}=132 K which is equivalent to a very small activation energy E_g/m, with m being m=43.6. The dark current mechanism is unclear. It has been demonstrated that the amplifier glow can be reduced by using off-chip JFET's directly connected to the unbuffered output bypassing the on-chip source follower [5] . Figure 7 shows a dark exposure which is normalized to a dark current in units of e/sec. It was obtained from the difference of two nondestructive readouts taken 1750 and 8990 sec after reset. Since the glow is confined to the regions close to the output amplifiers and the dark current exhibits a strong temperature dependence it seems reasonable to suspect that glow is not dominating our dark current measurements. But further investigations using external JFET's will be carried out.

4.4.Readout Noise

First noise tests applying double correlated sampling have been performed with a large analog bandwidth of the data acquisition system. The rise time of the system was 270 nsec. This is faster than the buffered video output of the on-chip source follower which has a rise time of 3 µsec. The rms noise of 32 consecutive double correlated readouts was 24 e rms, which includes the noise of both readouts of the double correlated clamp. Dark exposures of 2.5 sec were used. This result is based on the measured integrating node capacity of 34 fF and not on the value of 20fF as quoted by the manufacturer. Our setup is still susceptible to noise pickup from the cryostat environment and shielding must be further improved.

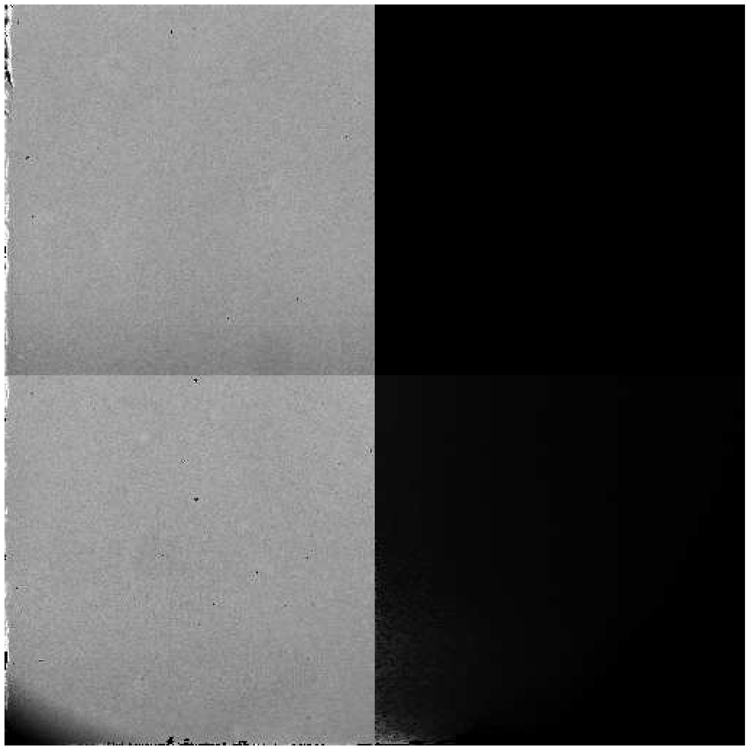

Figure 3 : K band quantum efficiency of Rockwell 1024x1024 HgCdTe array. Cut levels = 0 , 1. Mean QE is 64%.

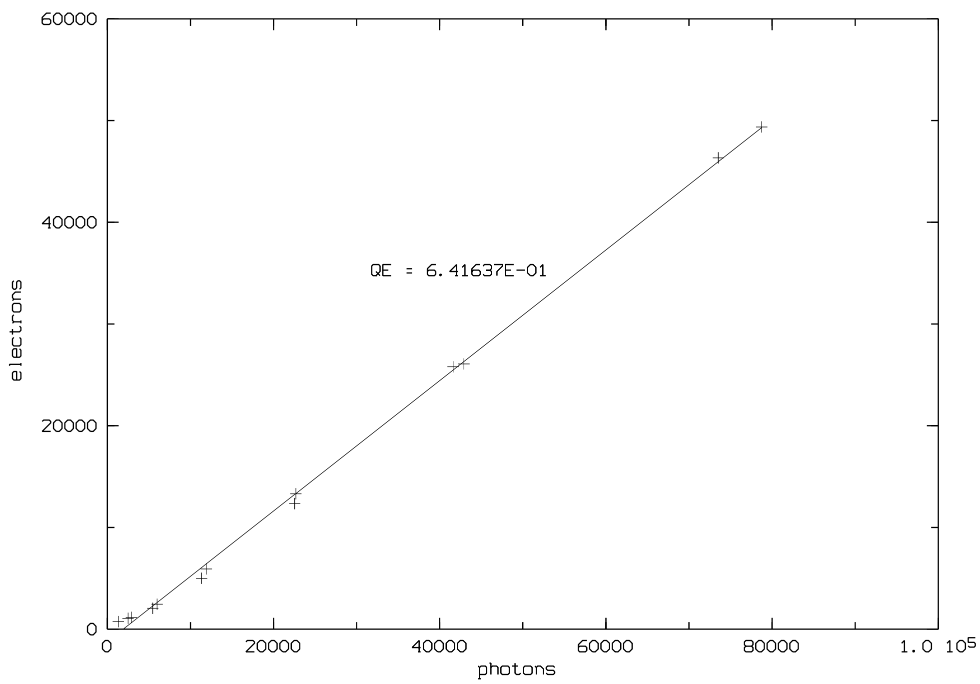

Figure 4 : Photometric quantum efficiency calibration of Rockwell 1024x1024 HgCdTe array in K band. Detector integration times 1 sec and 2 sec. External reverse bias voltage 500 mV.

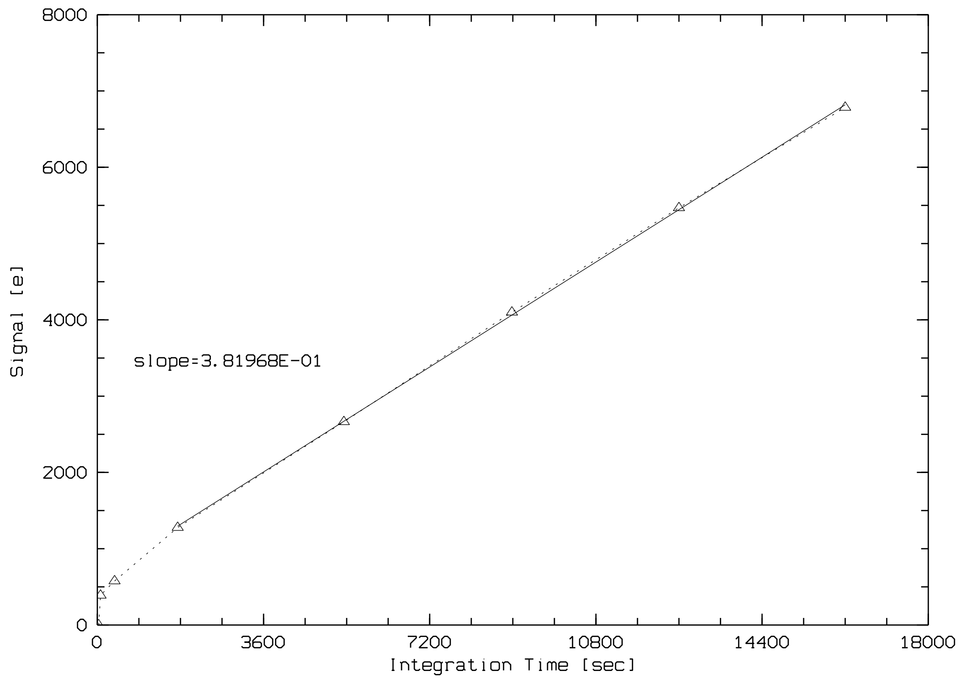

Figure 5 : Detector Signal versus time for a dark exposure at 55 K. Dark current is 0.38 e/sec.

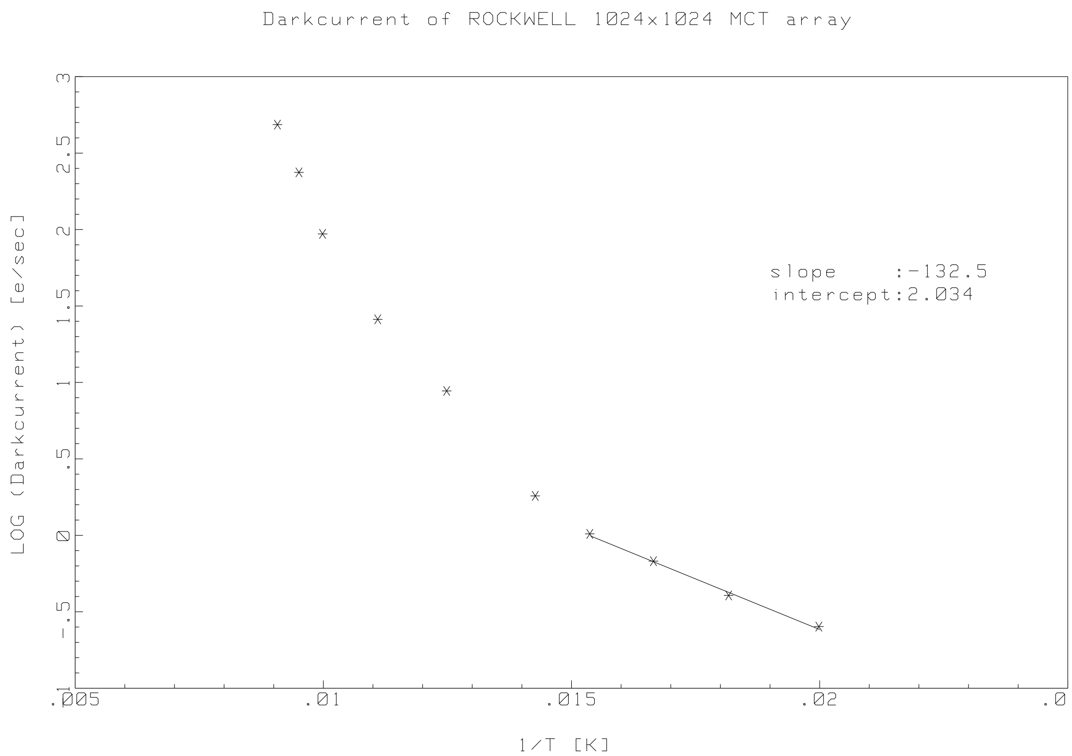

Figure 6 : Temperature dependence of dark current. Effective temperature at 50 K is T_{eff}=132 K.

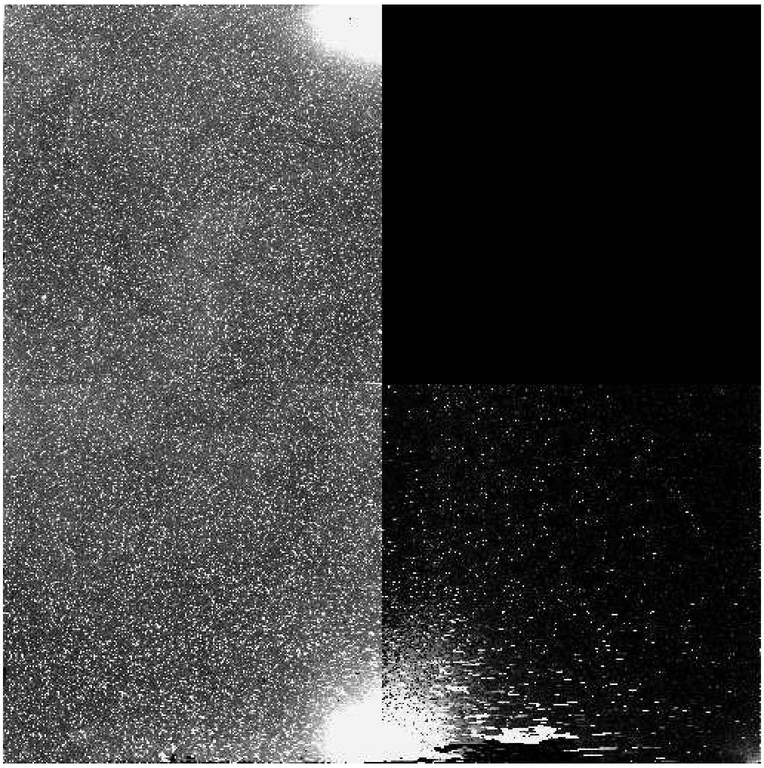

Figure 7 : Dark current of HAWAII 1024x1024 HgCdTe array. Low cut = 0 e/sec. High cut = 0.5 e/sec. Electroluminescence is confined to the corners of the quadrants.

In the multiple nondestructive sampling mode applying a least squares fit to 80 nondestructive readouts of the integration ramp of 2 minute dark exposures the readout noise could be reduced to 12 e rms in regions of the array at some distance from the buffer amplifiers and shift registers. Further tests are planned matching the analog bandwidth of the acquisition chain to the speed of the detector. External JFET's will be used bypassing the on-chip buffer output.

With measured readout noise and dark current figures of the HAWAII detector tested here, H band spectra having a spectral resolution R=2500 will be limited by the shot noise of the dark current and not by the readout noise, as soon as the detector integration becomes larger than 10 minutes. Simulations of both long slit spectrographs and integral field spectrometers predict for the OII line of a galaxy at z=2 a signal to noise improvement of a factor of 2 if the dark current is reduced from 900 e/sec/hour to 200 e/sec/hour.

4.5.Persistence

If the detector field of view contains a bright radiation source the subsequent dark exposures exhibit residual excess dark current of those pixels onto which the bright source had been imaged in the previous exposure. This persistence effect of the HAWAII device is strongly reduced in comparison to the NICMOS 3 array, the predecessor of the HAWAII detector [6] . The persistence effect is not completely eliminated in the HAWAII detector as demonstrated by a series of specific tests. In these tests a point source was imaged onto the detector and generated a total photocurrent of 2.2 10^5 e/sec. In the first subsequent 1 minute dark exposure the photocurrent was reduced to 200 e/sec. The second 1 minute dark exposure did not show any measurable residual excess dark current above the noise level of 10 e/sec.

4.6.Spot Scan

The sensitivity profile of a single pixel is required for modelling the overall MTF of the instrument including optics and detector. It helps the instrument designer to define the required optical quality. If the sensitivity profile of a single detector pixel is accurately known the mechanisms which reduce the quantum efficiency of the detector can be separated. The slope of the sensitivity profile yields the diffusion length of the minority carriers of the detector material. For these reasons a special effort was undertaken to produce an infrared spot which is small compared to the pixel size of 18.5 µm and can be used for spot scans of single pixels. Since the diameter of the airy disk is $2.44\lambda f^{\#}$ the f/11 Offner camera produces diffraction limited images which are larger than the pixel size. For this reason a special focal reducer lens f/11 to f/2 has been fabricated to produce light spots smaller than the pixel size. The lens had to fit in the converging beam of the f/11 Offner camera and occupies one of the filter wheel positions. The lens functions as substrate for the reflecting surfaces. The entrance and output surfaces of the lens are concentric to the object plane which is the detector surface. Therefore, the lens is totally achromatic independent of the detector material. The principle of the lens is a solid inverse cassegrain telescope. Figure 2 shows the first spot scan performed with this lens. The response of five adjacent pixels in a row is plotted versus spot position. The maxima of the response curves decrease from pixel to pixel because the scan direction is not parallel to the detector row. The upper curve is the total integrated intensity of all pixels. The next neighbors of the brightest pixel contain 15% of the signal measured on the central pixel. The energy concentrated on the central pixel is 60% of the total energy. The spot scan is probably a convolution of the optical spot profile and the detector response. The quoted values are worst case limits and further improvement of the optical alignment is necessary; This is difficult since the alignment has to be checked with pixels much larger than the optical spot diameter. The sensitivity profile of the detector is mainly determined by the diffusion length of the minority carriers. The location where the photon generates the signal charge is dependent on the absorption coefficient of the IR active material. The electron hole pair has to diffuse to the pn junction where it is separated by the electric field of the depletion region. Since the width of the depletion region depends on the bias voltage, the sensitivity profile may depend on the bias voltage.

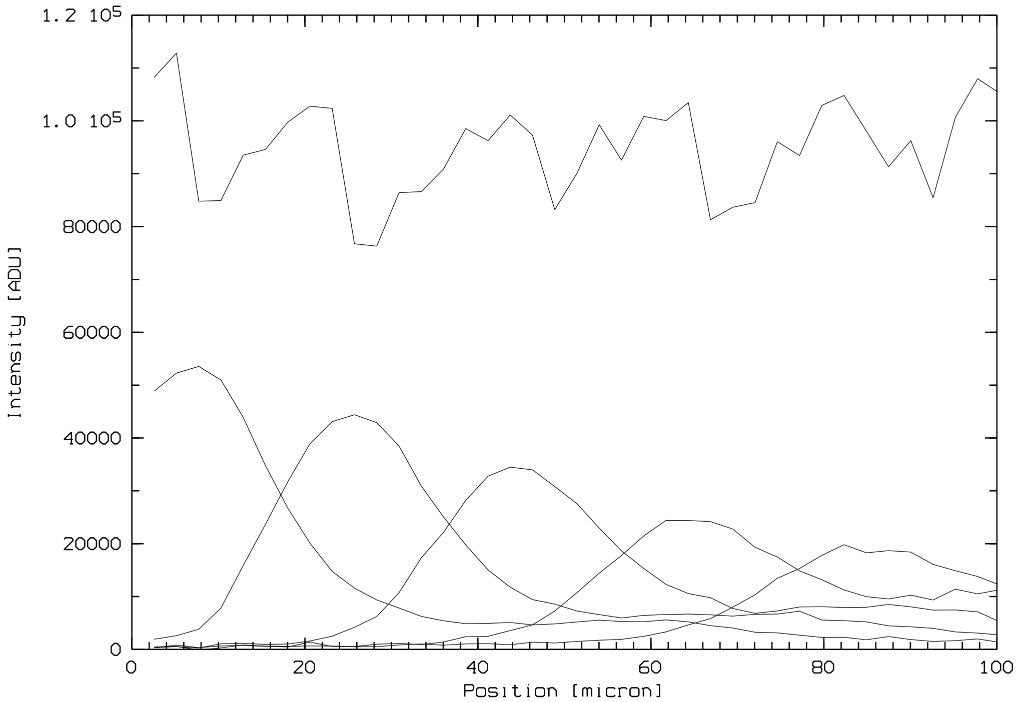

Figure 8 : Spot scan of HAWAII array.

4.7.Read speed and image sharpening

The low noise, low dark current and high quantum efficiency achieved with the HAWAII array open up new applications of the device as IR wavefront sensor [5] . Furthermore, at telescope foci without adaptive optics and tip tilt mirrors image sharpening can be achieved by on-chip tracking techniques [7] . In the multiple nondestructive readout mode the difference of two consecutive nondestructive readouts is a short time exposure with an integration time equal to the sampling interval. These short time exposures can be recentered to compensate for image motion induced by atmospheric turbulence. The time interval between two nondestructive readouts must be at least as long as the readout time τ of the array which is the critical parameter for these applications. To estimate the readout time τ required for the correction of image motion, a power spectral density of atmospheric tilt was used which is based on measured height profiles of wind speed and temperature turbulence coefficients C_T^2 [8] . In order to retrieve the phase variance of an image obtained from recentered differences of nondestructive readouts of integration time τ, the power spectral density must be multiplied by the filter function $1-(\sin(\pi\tau f)/\pi\tau f)^2$ and integrated over all frequencies f. An expression given by Parenti et al. [9] allows to convert the tilt corrected phase variance to Strehl ratios of images obtained with the on-chip tracking algorithm. For the multimode infrared instrument SOFI, which will be installed at the 3.5 m NTT telescope in LaSilla, the dependence of Strehl ratio on readout time τ achievable with on-chip tracking was calculated assuming typical seeing conditions of FWHM = 0.5 arcsec at λ = 0.5 µm and a wind speed of v = 5 m/sec. The result is shown in figure 9. Without any optimization we have been able to read the array with 3 µs address time per pixel. If all four quadrants are read out in parallel, this corresponds to a readout time of τ = 750 msec. In order to increase the speed of the output driver one can adjust the bias gate voltage from the nominal 3.5V setting towards ground. This will increase the current to the drive circuit. Unfortunately, one has to pay a dynamic range penalty for doing this. To overcome this problem one can adjust the detector substrate below ground. Further, the output source follower can be made faster by decreasing its pullup resistor. Experiments are ongoing, and we hope that a combination of these adjustments will enable us to do readouts faster. If the address time per pixel can be reduced to 1 µs the complete array can be read out in 250 msec. This would increase the Strehl ratio of K band images corrected by the on-chip tracking algorithm from 0.27 to 0.43.

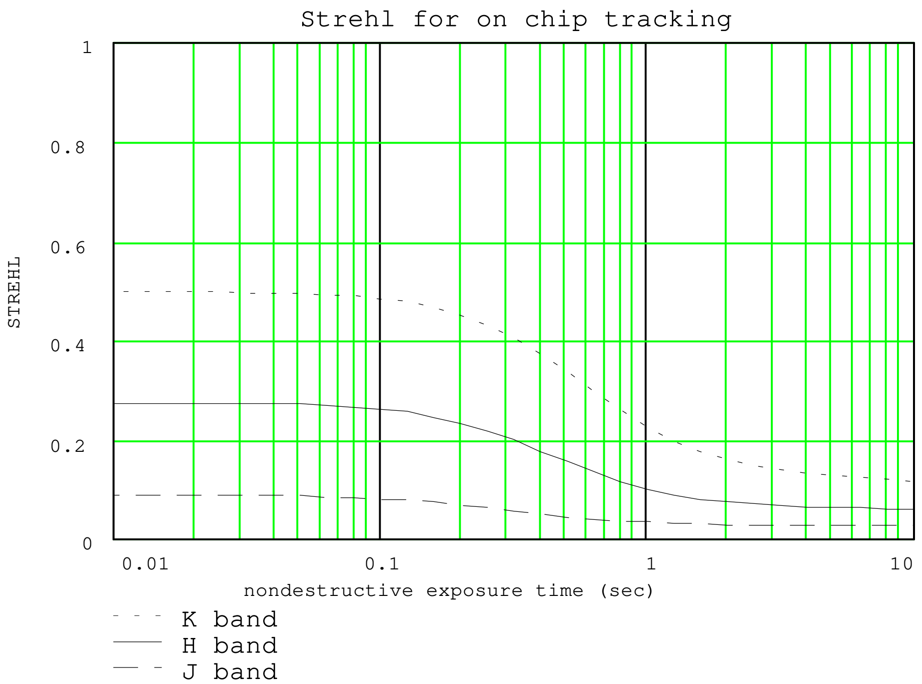

Figure 9 Strehl ratio of images corrected by on-chip tracking showing dependency on detector readout time τ for J, H and K band. Assumptions: telescope diameter 3.5 m, FWHM = 0.5 arcsec at λ = 0.5 µm, wind speed of v = 5 m/sec.

5.Conclusions

Megapixel IR arrays have become available and are under active investigation. The performance of an engineering grade HAWAII 1024x1024 HgCdTe array produced by Rockwell International Science Center has been evaluated in our new test camera. The array was operated by IRACE, our new ultrafast transputer based data acquisition system. The dark current of the HAWAII array is temperature dependent and 0.25e/sec at 50 K. Some of the problems such as amplifier glow and persistence encountered with NICMOS-3 arrays, the predecessor of the HAWAII array, have been substantially reduced. Readout noise of 12 e rms could be achieved but further improvements may be possible by better shielding and by using external JFET's bypassing the on chip amplifier. Readout times of 750 msec have been demonstrated. Experiments to reduce the readout time are in progress in order to increase the effectiveness of first order corrections of wavefront distortions induced by atmospheric seeing.

Our data acquisition system will be expanded to a 32 channel version for testing 1024x1024 InSb arrays produced by Santa Barbara Research Center. Large format 1Kx1K arrays are not yet off the shelf devices. However, plans already exist to extend the PACE-1 technology of HgCdTe to formats of 2Kx2K. Infrared focal plane technology is still rapidly developing and will expand the frontiers of IR astronomy.

6.Acknowledgements

The authors wish to thank B. Delabre, B. Köhler, L. Nöethe, A. van Dijsseldonk and O von der Lühe for their support and helpful discussions.

7.References

[1]A. M. Fowler, R. G. Probst, J.P. Britt, R. R. Joyce, F.C. Gillet, “Evaluation of an InSb Hybrid Focal Plane Array for Ground-based Astronomy”, Optical Engineering 26, 3, pp. 232-240, 1987.

[2]A. M. Fowler, I. Gatley, F.J. Vrba, H.D.Ables, A. Hoffman and J. Woolaway, “Aladdin, the 1024x1024 InSb Array: Test Results”, Proceedings SPIE 2475, pp. 27-33, 1995.

[3]L.J. Kozlowski, K. Vural, S.A.Cabelli, C.Y. Chen, D.E. Cooper, G.L Bostrup, D.M. Stephenson, W.L. McLevige, R.B.Bailey, K. Hodapp, D.Hall and W.E. Kleinhans, “2.5 µm PACE-I HgCdTe 1024x1024 FPA for Infrared Astronomy”, Proceedings SPIE 2268, pp. 353, 1994.

[4]M. Meyer, G. Finger and H. Mehrgan, “Connection between detector front end and number cruncher with 1 Gbit/s multiplexing fiber-optic link”, Proceedings SPIE 2475, pp. 97-104, 1995.

[5]K.W.Hodapp, J.L.Hora, L.L.Cowie, M.Metzger, E.Irwin, D.Hall, K. Vural, L.J. Kozlowski, S.A.Cabelli, C.Y. Chen, D.E. Cooper, G.L Bostrup, R.B. Bailey, W.E. Kleinhans, “The Hawaii Infrared Arrays: Testing and Astronomical Characterization of Prototype and Science-Grade Devices”, to be published in New Astronomy.

[6]G. Finger, P Biereichel, M. Meier and A.F.M. Moorwood, “Image Sharpening by On-Chip Tracking in IRAC2”, Proceedings SPIE 1946, pp. 134-145, 1993.

[7]G. Finger, P Biereichel, A. van Dijsseldonk, M. Meier and A.F.M. Moorwood, “Real Time Image Sharpening without Adaptive Optics by On-Chip Tracking”, Proceedings SPIE 2198, pp. 763-773, 1994.

[8]O. von der Lühe, M. Sarazin, “Power Spectral Densities of Atmospheric Image Wander at Paranal“, ESO Report VLT-TEL-92/2064, 1993.

[9]R.R. Parenti and R.J. Sasiela, “Laser-guide-star systems for astronomical applications”. Opt. Soc. Am., Vol 11, pp 288-309,1994.